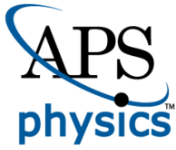

This is the accepted manuscript made available via CHORUS. The article has been published as:

Electrically tuning many-body states in a Coulomb-coupled InAs/InGaSb double layer

Xing-Jun Wu, Wenkai Lou, Kai Chang, Gerard Sullivan, Amal Ikhlassi, and Rui-Rui Du

Phys. Rev. B **100**, 165309 — Published 31 October 2019

DOI: 10.1103/PhysRevB.100.165309

Electrically tuning many-body states in a Coulomb-coupled InAs/InGaSb double layer

Xing-Jun Wu[1,*], Wenkai Lou[2], Kai Chang[2], Gerard Sullivan[3], Amal Ikhlassi[3], and Rui-Rui Du[1,4*]

[1] International Center for Quantum Materials, School of Physics, Peking University, Beijing 100871, China

[2] SKLSM, Institute of Semiconductors, Chinese Academy of Sciences, Beijing 100083, China

[3] Teledyne Scientific and Imaging, Thousand Oaks, California 91603, USA

[4] Department of Physics and Astronomy, Rice University, Houston, Texas 77251-1892, USA

[*]Email address: wxj_icqm@pku.edu.cn; rrd@rice.edu

Abstract: We study the transport properties of an electron-hole double layer consisting of barrier-separated InAs/InGaSb quantum wells. We focus on measurements of four- terminal resistivity of a Hall-bar sample as a function of electron (n)- and hole (p)- density, that are being tuned by a pair of top- and bottom- gates. In zero- magnetic field, we clearly observe an insulating phase which occurs at a charge neutral point, below a critical carrier density $n = p < 1 \times 10^{11} cm^{-2}$. This phase is characterized by a narrow and thermally-activated resistance peak and an anomalous Hall resistance. This observation reinforces our previous finding of an excitonic insulator. Remarkably, when the layer densities are being tuned into imbalance, here $p >> n$, a broader resistance peak emerges. We discuss this phase with respect to a possible (theoretically predicted) charge-density-wave ground state. Both phases can persist above ~25 K, indicating robust correlations in the electron-hole double layers.

At low enough temperature, interlayer Coulomb attraction in coupled electron-hole double layers (EHDL) would cause a pairing instability that leads to many-body phase transition when the typical distance between electrons (holes) within a layer approaches (or exceeds) the distance between the two layers. This many-body ground state includes charge density waves (CDW), Wigner crystals (WC) [1-5] and an excitonic phase [6-12] which may traverse the crossover from Bose-Einstein condensate (BEC) to a Bardeen–Cooper–Schrieffer-type state. Experimentally, pioneering works on quantum Hall electron (hole)-bilayer samples [13-18] revealed some vital features indicative of an excitonic phase transition to a Bose condensate at total filling fact of $\nu = 1$. Recently, many-body phase transition, in zero magnetic field, towards a condensed excitonic state was also reported [19-20]. Before interlayer pair correlation function g($\boldsymbol{r}$ = 0) actually diverges to form a bound exciton state in EHDL, where $\boldsymbol{r}$ is the projection of the electron-hole spacing parallel to the layers, calculations within the Singwi-Tosi-Land-Sjölander (STLS) approach point out that CDW instability would always occur with a divergence of in-phase static susceptibility [1, 5]. This means that transition to a CDW state in electron-hole liquids maybe is a precursor to the onset of the excitonic bound state. Experimentally, there have not yet been much reports about the many-body phase transition towards the zero-magnetic-field CDW state in EHDL. One possible effect attributed to this CDW state that we find is the observation of a collective insulating state in an EHDL made of high mobility GaAs/AlGaAs, which occurs at imbalanced layer densities [21].

The quantum spin Hall (QSH) insulating state has been realized in InAs/GaSb quantum well (QW) [22-24], which attracts much attentions in the past decade due to its time reversal symmetry (TRS) -protected helical edge modes. This state essentially can be well described by single-particle theory. In addition, due to the unique inverted band structure in InAs/GaSb, with

finite overlap of the InAs conduction band and GaSb valence band, electrons and holes could coexist in this structure, but partially confined in respective InAs or GaSb QW. Thus, a many-body instability is predicted theoretically for the ground state in this novel EHDL structure [9-11, 20,25]. Then, a question arises: are there any many-body phase transitions that could be observed experimentally in InAs/GaSb, and if any, do these many-body ground states still remain nontrivial topological phase? As topological excitonic insulator state is revealed in strongly hybridized InAs/GaSb [20], in this article, we present the result of electrical transport in an EHDL made of strained-layer InAs/InGaSb separated by 10-nm-thick AlSb middle barrier.

Our sample wafer was grown by molecular-beam epitaxy, consisting of 9.5 nm InAs, 10 nm AlSb, and 5 nm $In_{0.25}Ga_{0.75}Sb$ sandwiched between $Al_{0.7}Ga_{0.3}Sb$ barrier layers as depicted in FIG. 1a. Some changes have been made in this material: (1) Contrast with InAs/GaSb system [20], here, the GaSb layer is replaced by a ternary compound $In_{0.25}Ga_{0.75}Sb$, and the compressive strain (~ 1%) [22] in growth plane leads to a reduced mass for hole carriers, hence making a better match with the electron mass in InAs for exciton pairing. (2) By inserting a 10-nm-thick AlSb barrier between InAs and InGaSb QWs, the interlayer tunneling should be negligibly small while the interlayer correlations not largely affected (see, Ref. [25]). Fig. 1b shows the corresponding results of the band alignment calculated by eight-band $k \cdot p$ model. It can be found that, by inserting a 10-nm-thick middle barrier, the hybridization gap is closed as expected at the crossing points between the electron and hole dispersion relations. The sample in this work was wet-etched into a standard Hall bar of 40μm × 20μm size, and then thinned to about 1 μm using "flip-chip" process [26]. Aluminum layers were evaporated on both sides as dual gates, and ohmic contacts were made by depositing Indium with annealing (see Supplemental Material [27]). In such dual-gated Hall bar devices, the chemical potential and charge states can be fine-

tuned to the dilute limit. The low-temperature electron (hole) density at zero gate biases is $8 \times 10^{11} cm^{-2}$ ($7 \times 10^{11} cm^{-2}$) with an electron (hole) mobility ~ 10^5 $cm^2 V^{-1} s^{-1}$ (10^4 $cm^2 V^{-1} s^{-1}$). We perform standard four-terminal measurements in this work. Longitudinal resistance R_{xx} and Hall resistance R_{xy} are measured at the same time by a low-frequency lock-in setup.

Electrically tuning insulating phases in Coulomb-coupled EHDLs. To describe the charge states in the EHDL, we map the measured R_{xx} as a function of top gate bias (V_{TG}) and back gate bias (V_{BG}) in FIG. 1c. We classify the resistance behavior into three regimes. In regime I where there are more electrons than holes ($n > p$), the R_{xx} exhibits a peak upon sweeping the V_{BG} at a fixed V_{TG} (see, e.g., the blue curve at V_{TG} = -0.7 V). This feature can be understood by considering a charge compensation mechanism between the electron layer (InAs) and the hole layer (InGaSb) under the gate electrostatic potential. Specifically, as one sweeps much positive bias on V_{BG}, while holes are being depleted in the InGaSb, electrons will be accumulating in the InAs layer as well due to an imperfect screening by the hole layer, a resistance peak appears then in the crossover point. Moreover, the peak maximum increases consecutively as the V_{TG} is being set more negative (i.e., smaller n). This results in a ridge-like R_{xx} pattern running along the V_{TG} axis. In fact the R_{xx} can be calculated by the Drude conductivity of a two carrier system. Analogously, in the hole dominating regime II ($n < p$), a resistance ridge runs along the V_{BG} axis and peak values increases towards more positive V_{BG}. The resistances on the two ridges are in the range of 0.1 to 10 $k\Omega$. The positions of all these peaks are marked by blue dots in FIG.1c.

In what follows we will focus on regime III, where both n and p fall below ~$1 \times 10^{11} cm^{-2}$. The two resistance ridges merge and the pattern evolves into highly resistive peaks, R_{xx} > 100 $k\Omega$. In general there exists a pair of resistive peaks in this regime, which we term main peak or side peak respectively. For example, when keeping a constant V_{TG} = -1.1V and sweeping the V_{BG}

bias, we observe a pair of peaks as represented by the right end of the green curve. As will become clear in the following analysis, while these two peaks do overlap in the V_{TG}-V_{BG} map, they are distinctive in transport properties, implying driven by two distinctive origins.

FIG. 2 shows the main features of R_{xx} peaks: 1) FIG.2a describes the evolution of peaks as we sequentially reduce the electron density n (by more negative V_{TG} from -0.8 V to -1.25 V, total density change $\Delta n \sim -3 \times 10^{11} cm^{-2}$). The ensuring main R_{xx} peak grows from 2.5 to ~200 $k\Omega$ and a side peak emerges. Such a dramatic density dependences signal a critical behavior. 2) For the lowest n studied here, the onset of the main peak (side peak) is close to 40 K (15K), of an exceptionally large energy scale, indicating it should be associated with a condensate. This is further quantitatively confirmed by fitting the peak values into $R_{xx} = R_o \exp(-\Delta/2k_B T)$, where k_B is the Boltzmann constant. We find respectively for the main peak (the side peak) energy gap Δ_1 ~ 94 K ($\Delta_2 \sim 26$ K) by fitting the high T portion of the data.

Another major feature to distinguish these two insulating states is to concern the "line shape". Referring to FIG. 2e and 2f, we find that 1) For the main peak: while the peak value changes from ~ 40 to ~ 230 $k\Omega$ as the electron density n is being reduced, its center only shifts slightly towards more positive V_{TG} (i.e., p is almost unchanged). In other words, the main peak state is dominated by holes, and its HWHM is $\xi_1 \sim 0.67$ V. 2) For the side peak: while peak value changes from ~ 10 to ~ 80 $k\Omega$, the center tracks n, or in other words, the peak always occurs around charge neutrality (see below), with a narrower HWHM $\xi_2 \sim 0.24$ V. We can first rule out the possibility that these insulating states arise from interlayer tunneling. With applying $B_{//}$, the electron and hole dispersion relations would induce a relative shift proportional to their relative displacement in real space Δz. The regions where electron-hole band mixing exists would move

away from the Fermi energy [28] and thus the resistance peak is expected to decrease. This is contrary to our observation (see Supplemental Materials [27]).

Magneto-transport features of the insulating phases in dilute carrier regime. In the top panel of FIG. 3, we plot the p and n as a function of V_{BG} while fixing the V_{TG} at -1.2 V. We identify the three regimes of interest here. 1) Hole dominating regime: $p >> n$ and $p > n$, within which the Hall resistance R_{xy} across zero at $V_{BG} \sim 5.8$ V. In the two carrier model, this corresponds to the transport condition described by $\mu_e \cdot n - \mu_h \cdot p \ \approx \ 0$, and hence $p > n$ because of the fact that $\mu_e > \mu_h$. 2) Charge neutral regime: $n \ \approx \ p$. With more positive V_{BG}, the layer densities are tuned matched, as marked by a vertical band of red color, $n \ \approx \ p = \ (2.5 \pm 0.5) \times 10^{10} cm^{-2}$. In this regime, the typical distance (ℓ~63 nm) between electrons (holes) within a layer largely exceeds the distance between two layers(d~10 nm), thus, interlayer interaction would prevail. 3) Electron dominating regime, $p < n$: as V_{BG} increases and the holes are being further depleted, electrons will start to accumulate due to an imperfect screening by the hole layer, as marked by the n data points (red triangle) determined from the electron Shubnikov-de Haas (SdH) oscillation period in high magnetic fields.

In the charge-neutral regime, we clearly find the Hall resistance suddenly develops an anomalous dip as the side insulating state appears. This interesting observation should be related to the formation of excitonic state. Since exciton is charge neutral, it would not experience Lorentz force in B and thus Hall resistance should vanish. Moreover, the R_{xx} peak value and the depth of the R_{xy} dip grow as the perpendicular magnetic field $B_{\perp}$ increases, consistent with the prediction that B is expected to enhance the confinement and, hence, the exciton binding energy. However, the R_{xy} dip value here does not equal to zero and increases with $B_{\perp}$, away from a perfect exciton Bose-condensate. This arises from partly condensed electron-hole pairs: system

condenses only partly in electron-hole pairs, whereas parts of the system remain in the normal semi-metallic state, i.e., "unpaired" electrons and holes. This generally has two possibilities: 1) Anisotropy-induced electron-hole Fermi surface mismatch [29]. By using compressive strained materials and tuning the charge neutrality density sufficiently small, this effect should be small. 2) Scattering from short-range disorders [30], e.g. impurities, surface roughness. Exciton Bose-condensate is sensitive to short-range scattering, any short-range scattering process would change the momentum of electron and hole gases not identically, leading to a pair-breaking effect [30,31]. Considering this effect, we find that, the ratio of electron Drude transport lifetime($\tau_e = 1.3ps$) to quantum lifetime ($\tau_q = 0.12ps$) is $\tau_e/\tau_q \sim 11$, one order of magnitude larger than that in short-range scattering samples [32], indicating scattering from short-range disorders should be weak. Meanwhile, the scattering time τ for holes (electrons) is $\tau_h = 0.54ps$ ($\tau_e = 1.3ps$). While based on the pair-breaking condition as given by $\hbar/\tau > (\pi/2\gamma_e)k_B\mathrm{T}_c$ [30], where γ_e is Euler constant, k_B is Boltzmann constant, and $\mathrm{T}_c \sim$ 26 K deduced from above, the critical collision time τ_c at which pair-breaking effect begins is $\tau < \tau_c = 0.1$ps, smaller than $\tau_{h(e)}$ but on the same order of magnitude with τ_h. Therefore, it follows that scattering from a few short-range disorders probably leads to "unpaired" electrons and holes that give rise to a non-zero R_{xy} increasing with B.

We then estimate the likelihood of exciton BEC for the side insulating state. Using the eight-band $k \cdot p$ method we have calculated the electron effective mass m_e*= $0.039m_0$ ($m_0 = 9.11 \times 10^{-31}kg$), and the hole effective mass $m_h^* = 0.095m_0$. We note here m_e^* shifts upward from 0.03 m_0 in unstrained InAs while the m_h^* shifts downward from $0.3m_0$ in unstrained GaSb [33], confirming that strained-layer InAs/GaInSb offers a more symmetrical electron-hole system. Within the effective mass approximation, taking a dielectric constant $\varepsilon \sim 14$ and an interlayer

distance (measured between the centers of electron and hole quantum wells) $d = 17.2\ nm$, we estimate a 2D exciton Bohr radius a_B = 11 nm. By taking $n_0 \cdot \pi r_{avg}^2 = 1$ and $n_0 = 2.5 \times 10^{10} cm^{-2}$, we estimate an average in-plane intra-exciton distance $2r_{avg}$ = 70 nm and arrive at a dimensionless density $r_d = \frac{r_{avg}}{a_B} \approx 3.2$, indicating an exciton BEC regime. We comment that since screening effect is neglected here, a_B is somewhat under estimated, in reality the system may shift towards the BEC - BCS crossover, but still on the BEC side [34-38].

Possible charge density wave state at imbalanced layer densities. Another interesting observation is that the main insulating state occurs at a charged state of imbalanced electron-hole densities before the onset of excitonic bound state. Specifically, referring to FIG. 3a we find the R_{xx} peak appears around $p : n \approx 3:1$. This insulating phase can also be found in some other unstrained barrier-separated InAs/GaSb wafers. The unimportance of $n = p$ precludes an excitonic origin and a new mechanism is required for this main insulating state. It is interesting to note a similar insulating phase found in a high mobility GaAs EHDL with an equal layer spacing [21]. The transition to the insulating phase does not depend on the matching of the layer densities, while emerges also at around p ≈ 3n in its instance ($p = 1.6 \times 10^{11} cm^{-2}, n = 4{\sim}6 \times 10^{10} cm^{-2}$). A CDW phase is suggested for this state.

In Coulomb-coupled EHDL, collective excitation modes can be given by the poles of the dielectric function $\epsilon^{-1}(q, \omega)$. Any value of (q, ω) makes a singular ϵ^{-1}, that describes the onset of a collective excitation mode where density modulation can be spontaneously developed and the charge susceptibility diverges at these (q_0, ω_0). If $q_0 \neq 0$ and $\omega_0 = 0$, a collective mode with a periodic density modulation of wavevector q_0 can be developed without any energy required. This zero energy mode is a CDW or WC ground state, depending on q_0 at which the

divergence occurs. This collective motion is easily to be pinned by any background disorder [39], thus could create an insulating state. This CDW instability is expected to occur in the EHDL before the onset of excitonic bound states [5], which is consistent with our observation. On the other hand, we notice that the hole layer alone would not form a WC state: taking $m_h^* = 0.095m_0$ and $p \sim 7.5 \times 10^{10} cm^{-2}$, we have Bohr radius $a_{B,h}$* = 9 nm for holes, and layer density $r_s^* = (\pi p)^{-1/2} / a_{B,h}^* = 2.3$ for $d/a_{B,h}^* = 1$, where d is the interlayer separation. This result can be compared with the STLS calculations of a symmetric EHDL [5] which show that the critical layer density for a CDW phase is about $r_s = 4$ for $d/a_B^* = 1$. Considering mass asymmetry and finite layer width effects in real EHDL system, the critical layer density for the CDW phase transition is expected to be enhanced greatly [40] and, thus, a lower r_s is expected. Path integral Monte Carlo simulation [41] gives an intuitive description for the CDW state in mass-asymmetric EHDLs, that in the presence of electrons, the hole arrangement started developing density modulations in real space while the lighter electrons remained in a nearly homogeneous state. The heavier holes are comparatively more correlated than the electrons, and thus, dominate the overall ground-state behavior. This is consistent with the observation in Fig. 2(f) that the center of the main insulating state is largely dominated by the holes. As the electron density are being further reduced, the electron arrangement changes from nearly homogeneous to localized, and ultimately, certain broken symmetry order could be stabilized by forming a CDW phase of a specific configuration such as a triangular structure, where one electron is being screened by three neighboring holes.

Nonlocal transport measurement of the insulating phases. Nonlocal transport measurement has been a useful tool to prove the presence of conducting edge channels in two-dimensional topological insulator [42]. Such nonlocal transport has been experimentally observed in broken-

gap InAs/GaSb [43], indicating the existence of helical edge channels in the topological insulating phase. By suppressing the interlayer tunneling amplitude, the topological property in InAs/GaSb is anticipated to be changed [44, 45]. To explore the topology nature of these two many-body insulating phases, two sets of current paths are taken as shown in Fig. 4, i.e., current path I (I_{14}: 1 in, 4 out) and path II (I_{23}: 2 in, 3 out), and the voltage drops (V_{56}) between the same leads (lead 5 and lead 6) are recorded at the same time. Fig. 4(a) shows the V_{BG} dependence of $R_{14,56}$ and $R_{23,56}$ at fixed V_{TG} = -1.2V, where $R_{14,56} = V_{56}/I_{14}$ and $R_{23,56} = V_{56}/I_{23}$. We find the transport of the insulating phases satisfies bulk transport, $R_{14,56} \approx R_{23,56}$, exhibiting a local resistivity. By contrast, the existence of edge states would necessarily lead to nonlocal transport, then the relation, $R_{14,56} \approx R_{23,56}$, would be no longer met which can be seen from the corresponding equivalent circuit diagram of edge channel in Fig. 4(b) according to the Landauer − Büttiker formalism [46].

Specifically, assuming that the edge channel is present in the insulating phases, the resistance R_{56} can then be given by a parallel resistance model, $1/R_{56} = 1/R_{edge} + 1/R_{bulk}$, where R_{edge} comes from edge channel conductivity and R_{bulk} from the residual bulk conductivity. Different current paths presented in Fig. 4(b) would cause different edge channel resistance R_{edge} between lead 5 and 6 (e.g., R_{edge}=R_0 for path I and R_{edge}=$R_0/2$ for path II, R_0 is the 25μm-long edge channel resistance), while R_{bulk} remains unchanged. Thus, R_0 can be extracted from these two current paths. Take the side insulating phase as an example, $R_0 \sim 159\mathrm{h}/\mathrm{e}^2$. This means the coherence length (a length scale at which edge transport is dissipationless) λ_φ is about 160 nm, which is at least one order of magnitude smaller than previously reported in topologically protected edge states in InAs/GaSb QSH regime [22,24]. This observation implies the topology in the side insulating phase may have been changed compared to the QSH

insulating phase by suppressing the interlayer tunneling. A similar analysis can also be used for the main insulating phase. In fact, this is an interesting result in light of the phase transition between topological and non-topological states in EHDL. Interlayer tunneling plays important roles in formation of quantum spin Hall effect, exciton condensation, and other emergent quantum phases [44, 45]. In addition to tuning the carrier densities by gates, future experiments by tuning interlayer tunneling, using a middle barrier of different barrier height and thickness, should enable a quantitative study on the emergence of topological properties in this system.

In summary, we have experimentally observed many-body phases in Coulomb-coupled InAs/InGaSb double layer. By electrically tuning dual gates, we are able to tune many-body phase transitions. The side insulating state emerges around total charge neutrality and shows features of an excitonic phase, while the main insulating state occurs at imbalanced layer densities before the onset of excitonic state, and we attribute it to a CDW phase. Moreover, both insulating phases become topological trivial with a negligibly-small interlayer tunneling amplitude. Remarkably, this work opens the experimental studies of many-body phase transitions in Coulomb-coupled EHDL, and helps us to build up a rich phase diagram including many-body phases and the topological phase in InAs/GaSb.

Acknowledgements

We thank Fei Xue, A. H. MacDonald, Changli Yang, L. H. Hu, and Congjun Wu for helpful discussions. The work at Peking University was financially supported by National Key R and D Program of China (2017YFA0303301). The work at Rice University was funded by NSF Grant No. DMR-1508644 and Welch Foundation Grant No. C-1682. WKL and KC were supported by NSFC (Grant No. 11434010).

References and Notes:

1. Lerwen Liu, L. Swierkowski, D. Neilson and J. Szymanski, Static and dynamic properties of coupled electron-electron and electron-hole layers. *Phys. Rev. B* **53**, 7923 (1996).
2. L. Swierkowski, D. Neilson and J. Szymanski, Enhancement of Wigner crystallization in multiple-quantum-well structures. *Phys. Rev. Lett.* **67**, 240 (1991).
3. R. K. Moudgil and G. Senatore, Dynamic correlations in symmetric electron-electron and electron-hole bilayers. *Phys. Rev. B* **66**, 205316 (2002).
4. S. De Palo, F. Rapisarda, and Gaetano Senatore, Excitonic condensation in a symmetric electron-hole bilayer. *Phys. Rev. Lett.* **88**, 206401(2002).
5. Lerwen Liu, L. Swierkowski and D. Neilson, Excition and charge density wave formation in spatially separated electron-hole liquids. Physica B **249**, 594(1998).
6. For an earlier review, See, *e.g.*, P. B. Littlewood and X. Zhu, Possibilities for exciton condensation in semiconductor quantum-well structures. *Physica Scripta.* **T68**, 56 (1996), and references there in.
7. C. Comte, P. Nozières, Exciton Bose condensation: the ground state of an electron-hole gas – I. Mean field description of a simplified model. *J. Phys.* **43**, 1069 (1982).
8. Yu. E. Lozovik and Y. I. Yudson, Feasibility of superfluidity of paired spatially separated electrons and holes; a new superconductivity mechanism. *Sov. Phys. JETP Lett.* **22**, 274 (1975).
9. S. Datta, M. R. Melloch, and R. L. Gunshor, Possibility of an excitonic ground state in quantum wells. *Phys. Rev. B* **32**, 2607(1985).
10. X. Xia, X. M. Chen, and J. J. Quinn, Magnetoexcitons in a GaSb-AlSb-InAs quantum-well structure. *Phys. Rev. B* **46**, 7212 (1992).
11. Y. Naveh, and B. Laikhtman, Excitonic instability and electric-field-induced phase transition towards a two-dimensional exciton condensate. *Phys. Rev. Lett.* **77**, 900 (1996).
12. X. Zhu, P. B. Littlewood, M. S. Hybertsen, and T. M. Rice, Exciton condensate in semiconductor quantum well structures. *Phys. Rev. Lett.* **74**, 1633 (1995).
13. J. P. Eisenstein and A. H. MacDonald, Bose-Einstein condensation of excitons in bilayer electron systems. *Nature* **432**, 691 (2004).
14. E. Tutuc, M. Shayegan, and D. A. Huse, Counterflow Measurements in Strong Correlated GaAs Hole Bilayers: Evidence for Electron-Hole Pairing. *Phys. Rev. Lett.* 93, 036802 (2004).

15. Y. Yoon, L. Tiemann, S. Schmult, W. Dietsche, K. von Klitzing, and W. Wegscheider, Interlayer tunneling in couterflow experiments on the excitonic condensate in quantum Hall bilayers. *Phys. Rev. Lett.* **104**, 116802 (2010).
16. D. Nandi, A. D. K. Finck, J. P. Eisenstein, L. N. Pfeiffer, and K. W. West, Exciton condensation and perfect Coulomb drag. *Nature* **488**, 481 (2012).
17. X. Liu, K. Watanabe, T. Taniguchi, B. I. Halperin, and P. Kim, Quantum Hall drag of exciton condensate in graphene. *Nat. Phys.* **13**, 746 (2017).
18. J. I. A. Li, T. Taniguchi, K. Watanabe, J. Hone, and C. R. Dean. Excitonic superfluid phase in double bilayer graphene, *Nat. Phys.* **13**, 751 (2017).
19. G. William Burg, Nitin Prasad, Kyounghwan Kim, Takashi Taniguchi, Kenji Watanabe, A. H. MacDonald, L. F. Register, and E. Tutuc. Strongly enhanced tunneling at total charge neutrality in double-bilayer graphene-WSe2 heterostructures. Phys. Rev. Lett. 120, 177702 (2018).
20. L. J. Du, Xinwei Li, W. K. Lou, Gerard Sullivan, K. Chang, J. Kono, and Rui-Rui Du, Evidence for a topological excitonic insulator in InAs/GaSb bilayers. *Nature Comm.* **8**, 1971 (2017).
21. A. F. Croxall, K. Das Gupta, C. A. Nicoll, H. E. Beere, I. Farrer, D. A. Ritchie, and M. Pepper, Possible effect of collective modes in zero magnetic field transport in an electron-hole bilayer, *Phys. Rev.B* **80**, 125323 (2009).
22. L. J. Du, T. X. Li, Wenkai Lou, Xingjun Wu, Xiaoxue Liu, Zhongdong Han, Chi Zhang, Gerard Sullivan, Amal lkhlassi, Kai Chang, and Rui-Rui Du, Tuning Edge States in Strained-Layer InAs/GaInSb Quantum Spin Hall Insulators, *Phys. Rev. Lett.*, **119**, 056803 (2017).
23. C. X. Liu, T. L. Hughes, X. L. Qi, K. Wang, and S. C. Zhang, Quantum spin Hall effect in inverted type-II semiconductors. *Phys. Rev. Lett.* **100**, 236601 (2008).
24. I. Knez, R. R. Du, and G. Sullivan, Evidence for helical edge modes in inverted InAs/GaSb quantum wells. *Phys. Rev. Lett.* **107**, 136603 (2011).
25. Xingjun Wu, W. K. Lou, K. Chang, Gerard Sullivan, and Rui-Rui Du, Resistive signature of excitonic coupling in an electron-hole double layer with a middle barrier. *Phys. Rev. B* **99**, 085307 (2019).

26. M. V. Weckwerth, J. A. Simmons, N. E. Harff, M. E. Sherwin, M. A. Blount, W. E. Baca, and H. C. Chui, Epoxy bond and stop-etch (EBASE) technique enabling backside processing of (Al)GaAs heterostructures, *Superlatt. Microstruct.* **20**, 561 (1996).
27. See Supplemental Material at [URL] for device processing details and in-plane magnetic-field dependence.
28. M. Lakrimi, S. Khym, R. J. Nicholas, D. M. Symons, F. M. Peeters, N. J. Mason, and P. J. Walker, Minigaps and novel giant negative magnetoresistance in InAs/GaSb semimetallic superlattices. *Phys. Rev. Lett*. **79**, 3034 (1997).
29. J. Zittartz, Anisotropy effects in the excitonic insulator. *Phys. Rev.* **162**,752 (1967).
30. J. Zittartz, Theory of the Excitonic Insulator in the Presence of Normal Impurities, *Phys. Rev.* **164**, 575 (1967).
31. R. Bistritzer, A. H. MacDonald, Influence of Disorder on Electron-Hole Pair Condensation in Graphene Bilayers, *Phys. Rev. Lett.* **101,** 256406 (2008).
32. S. Das Sarma, F. Stern, Single-particle relaxation time versus scattering time in an impure electron gas, *Phys. Rev. B* **32**, 8442 (1985).
33. N. Bouarissa, H. Aourag, Effective masses of electrons and heavy holes in InAs, InSb, GaSb, GaAs and some of their ternary compounds. *Infrared Phys. Technol.* **40**, 343 (1999).
34. N. F. Mott, The transition to the metallic state. *Phil. Mag.* **6**, 287 (1961).
35. R. S. Knox, Solid State Physics, edited by F. Seitz and D. Turnbull (Academic Press, New York, 1963), Suppl. **5**, p. 100.
36. L. V. K. Keldysh and Y. V. Kopaev, Possible instability of the semimetallic state toward coulomb interaction. *Sov. Phys. Solid State* **6**, 2219 (1965).
37. D. Jérome, T. M. Rice, and W. Kohn, Excitonic insulator. *Phys. Rev.* **158**, 462 (1967).
38. B. I. Halperin and T. M. Rice, Possible anomalies at a semimetal-semiconductor transition. *Rev. Mod. Phys.* **40**, 755 (1968).
39. G. Grüner, The dynamics of charge-density waves, *Rev. Mod. Phys*. **60**, 1129 (1988).
40. R. K. Moudgil, Coupled electron-hole quantum well structure: mass asymmetry and finite effects, *J. Phys.: Condens. Matter* **18**, 1285 (2006).
41. P. Ludwig, A. Filinov, Yu. E. Lozovik, H. Stolz, M. Bonitz, Crystallization in mass-asymmetric electron-hole bilayers, *Contrib. Plasma Phys.* **47**, 335 (2007).

42. A. Roth, C. Brüne, H. Buhmann, L. Molenkamp, J. Maciejko, X. Qi, and S. C. Zhang, Nonlocal transport in the quantum spin Hall state, *Science* **325**, 294 (2009).
43. K. Suzuki, Y. Harada, K. Onomitsu, and K. Muraki, Edge channel transport in the InAs/GaSb topological insulating phase, Phys. Rev. B 87, 235311 (2013).
44. D. I. Pikulin and T. Hyart, Interplay of exciton condensation and the quantum spin Hall effect in InAs/GaSb bilayers. *Phys. Rev. Lett.* **112**, 176403 (2014).
45. Fei Xue and A. H. MacDonald, Time-reversal Symmetry Broken Nematic Insulators Near Quantum Spin Hall Phase Transitions. *Phys. Rev. Lett.* **120**, 186802 (2018).
46. M. Büttiker, Absence of backscattering in the quantum Hall effect in multiprobe conductors. *Phys. Rev. B* **38**, 9375 (1988).

FIG. 1. (a) shows a sketch of the InAs/InGaSb double layer separated by a 10-nm-thick AlSb middle barrier. Top and back gates are fabricated on both sides. **(b)** Band structure of InAs/AlSb/InGaSb double layer calculated using eight-band $k \cdot p$ method, for low carrier density. **(c)** shows four terminal longitudinal resistance R_{xx} as a function of top gate bias V_{TG} and back gate bias V_{BG} at 300mK. Blue dots correspond to the positions of the R_{xx} peaks. Three regimes of the charge states are marked along with the corresponding schematic diagram of band structures.

FIG. 2. (a) Longitudinal resistance R_{xx} measured at temperatures between 4.5 and 40 K for V_{TG} = -1.25, -1.1, -0.8 V, respectively. **(b)** Temperature dependence of the main peak at V_{TG} = -1.25, -1.1, -0.8 V, respectively. Here R_{xx} are multiplied by 3 and by 20 in the latter two cases for clarity. Estimated Energy gap are ~94 K, ~53 K respectively at V_{TG} = -1.25 and -1.1 V. **(c)** Temperature dependence of the side peak at V_{TG} = -1.25 V, and an energy gap of ~26 K is estimated. **(d)** R_{xx} as a function of V_{BG} at a fixed bias V_{TG}, shown by the solid line. The data are fitted by two extreme functions (red and green curves); blue dashed dot curve shows the overall fit. **(e), (f)** Fitting curves are shown for the side peak and the main peak, respectively.

FIG. 3. Magneto-transport results at V_{TG} = -1.2 V, T = 0.3 K. Top panel: the electron density n and the hole density p are displayed as a function of V_{BG}. Circles and triangles represent hole and electron densities respectively. Middle and bottom panels show R_{xx} and R_{xy} features at various perpendicular magnetic fields from 1.5 T to 4.5 T in steps of 0.5 T (see text).

FIG. 4. (a) Nonlocal transport results. **(b)** Two equivalent edge resistance circuit diagram based on Landauer – Büttiker formalism when current flows along different paths in a Hall-bar device. Here, R_0 represents the resistance of a 25μm-long edge channel as depicted in the inset of (a)

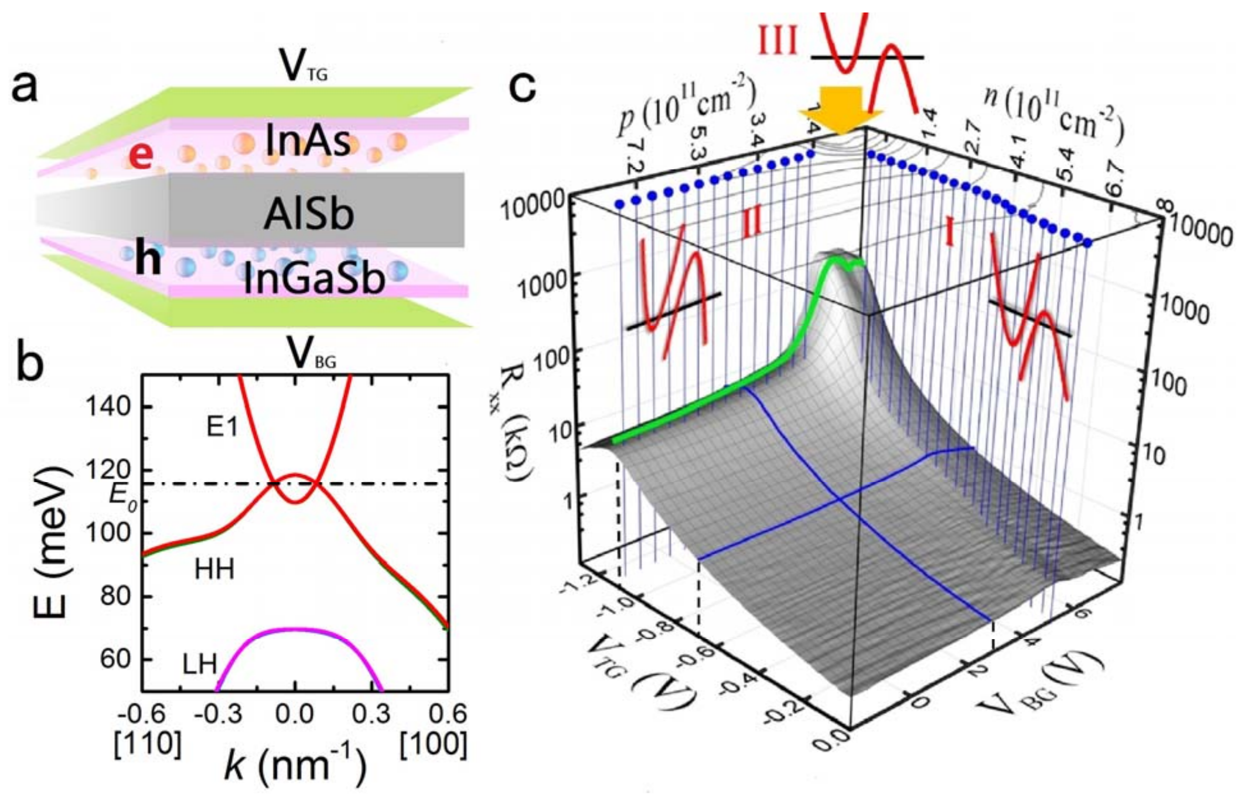

Figure. 1

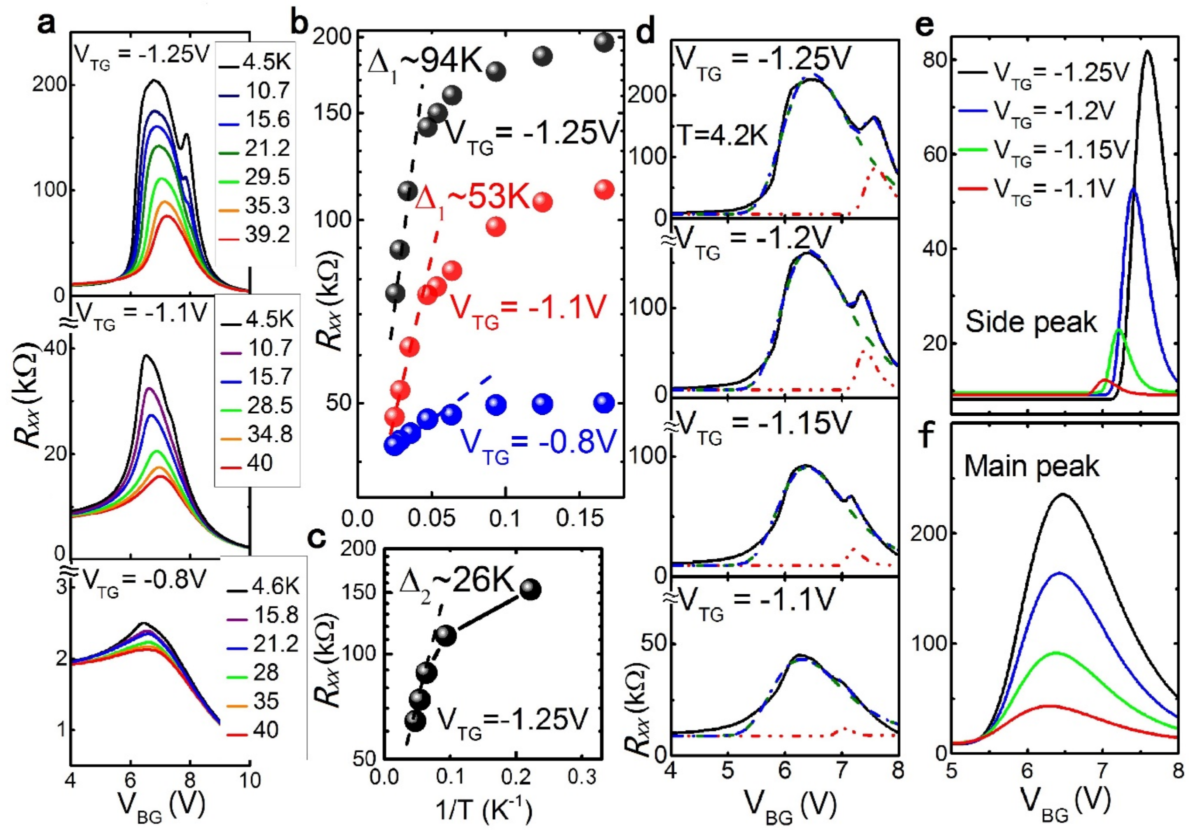

Figure. 2

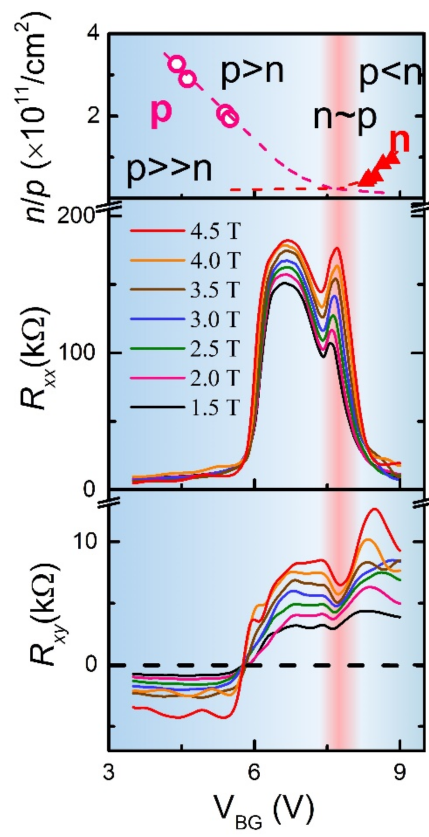

Figure. 3

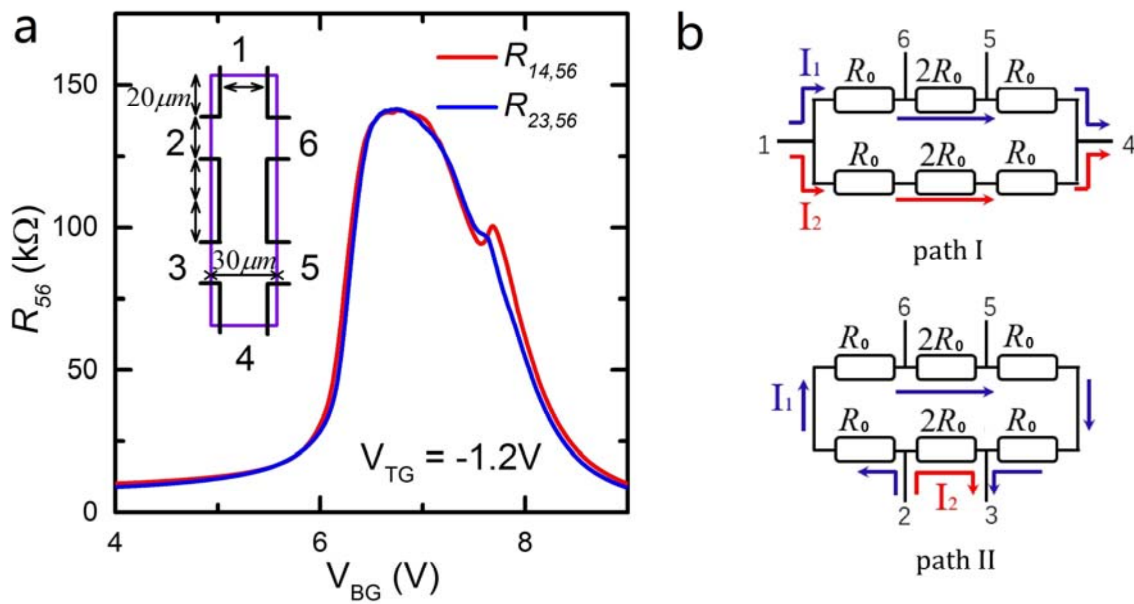

Figure. 4